Research Article

Impacts of Chemical Reaction and Suction/Injection on the Mixed Convective Williamson Fluid past a Penetrable Porous Wedge

Majid Hussain,[1] **Akhtar Ali,**[2] **Mustafa Inc** ,[3,4,5] **Ndolane Sene** ,[6] **and Muhammad Hussan**[2]

[1]*Department of Natural Sciences and Humanities, University of Engineering and Technology Lahore, Lahore 54890, Pakistan*
[2]*Department of Mathematics, Government College University, Faisalabad 38000, Pakistan*
[3]*Department of Computer Engineering, Biruni University, Istanbul, Turkey*
[4]*Department of Mathematics, Firat University, 23119 Elazig, Turkey*
[5]*Department of Medical Research, China Medical University, Taichung, Taiwan*
[6]*Laboratoire Lmdan, Departement De Mathematiques De Decision Universite Cheikh Anta Diop De Dakar,
BP 5683 Dakar Fann, Senegal*

Correspondence should be addressed to Mustafa Inc; minc@firat.edu.tr and Ndolane Sene; ndolanesene@yahoo.fr

The impacts of chemical reaction and suction/injection in Williamson fluid flow along a porous stretching wedge are discussed in the present paper. Recently, a lot of numerical and theoretical studies are accessible for illustrating the chemical reaction impact on non-Newtonian fluids with different geometries and conditions. Considering this fact, we inspect the heat transport behavior of Williamson fluid due to a stretching porous wedge with suction or injection. The governing PDEs are converted into ODEs with reliable similarity transformation. These ODEs are solved numerically by BVP4C based in MATLAB system, and the assessment of outcomes for the validation tenacity is presented in Table. Combined plots are sketched to discern the impact of dominant sundry parameters on the flow fields. Along with them, the Sherwood number, skin friction factor, and the rate of heat transfer are also bestowed in graphs.

1. Introduction

Numerous authors chose to work with non-Newtonian fluids rather than Newtonian fluids until they understood the applications of non-Newtonian models [1–3] in the era of bio sciences, material processing, food industries, ceramic products, wire coating, lubricants, polymeric liquids, detergents, engineering and petroleum industries, etc. Several constitutive models with various non-Newtonian models are presented in [4]. The Williamson model is a non-Newtonian fluid firstly introduced by Williamson [5]. The governing equations of this model describe the pseudo-plastic features of the fluids which piqued the interest of many researchers to work on Williamson fluid with different geometries and physical conditions. For instance, Malik et al. [6] searched the numerical results of Williamson fluid over a stretched cylinder in the presence of heat generation absorption and

variable thermal conductivity. Kumaran et al. [7] investigated the melting heat transfer phenomenon in MHD radiative flow of Williamson fluid in the existence of non-uniform heat source/sink. Hayat et al. [8] utilized modified Darcy's law on the flow of Williamson fluid in a channel. They achieved the solution using built-in ND-solver command in Mathematica software. Heat and mass transfer characteristics in 3D Williamson–Casson fluid past a stretching sheet had been highlighted by Raju et al. [9]. Noreen et al. [10] measured the performance of heat in electro-osmotic Williamson fluid past a microchannel.

Meanwhile, Subbarayudu et al. [11] revealed the time dependent assessment of radiative blood flow of Williamson fluid against a wedge. RK 4th order with shooting method was utilized by them to find the solution of the governing equations. Hussain et al. [12] highlighted the homogeneous-heterogenous reaction on the convective flow of Williamson

fluid over sheet and cylinder. Inquiry of variable conductivity, viscosity, and diffusivity on the magneto cross Williamson fluid had been analyzed by Salahuddin et al. [13].

Involvement of blowing or suction past a porous wedge/surface significantly changes the flow field behavior. Injection or withdrawal of fluid over a permeable bounding wedge/surface is of prodigious concern in everyday problems such as glazing of wires and film presentations, polymer fiber, coating, and so on. During the design of thrust bearing, thermal oil recovery, and radial diffusers, suction or injection plays a vital role. Numerous other researchers have successfully produced and discussed the results [14, 15] in the area of Darcian porous wedge/surface.

In chemical reactions, suction is useful to remove reactants, whereas blowing is useful to eliminate reactants, whereas blowing is advantageous to avoid corrosion, add reactants, and cool the wedge or shrink. Zahmatkesh et al. [16] investigated the entropy generation in axisymmetric stagnation flow of nanofluid through a cylinder with constant wall temperature and uniform suction blowing at the surface. Singh et al. [17] have considered the flow of micropolar fluid past a permeable wedge in the presence of Hall, ion slip current, and chemical reaction effects. Analytic solutions were achieved by implementing the differential transform method (DTM). Saleem et al. [18] discussed the blowing suction effects on temperature and velocity distribution of flow past a flat plate. They showed that factor of drag force enhanced with the increasing values of suction and reduced when blowing is applied.

The problem of chemical and diffusion reaction in a isothermal laminar flow along semi-infinite plate has been discussed by Fairbanks and Wike [19]. Ahmed et al. [20] provided the numerical and analytical solution to 3D channel flow in the existence of chemical reaction and sinusoidal fluid injection. Sulochana et al. [21] scrutinized the frictional heating on chemically reacting mixed convective Casson nanofluid past an inclined porous plate with radiation. Zaib et al. [22] made a numerical treatment of second law analysis of magnetocross nanofluid past a wedge with binary chemical reaction and activation energy. Nandi and Kumbhakar [23] scrutinized the chemical reaction and viscous dissipation effects on tangent hyperbolic nanoliquid over a stretching wedge with various conditions.

This discussion addressed the shortcoming flow of Williamson liquid bounded above the stretched porous wedge. The chemical reaction phenomenon is explained in this study. BVP4C [24–26] built-in MATLAB solver is used to solve the coupled non-linear equation. Impacts of sundry pertinent parameters are explained through graphs. The study of chemically reacting Williamson fluid over a stretchable porous wedge has not been discussed so far. The flow fields are characterized by expanding velocities, skin friction, and Sherwood and Nusselt number graphs. This work aims to provide basic ground for the researchers to explore the flow of the Williamson model over a porous wedge with chemical reaction.

In the current exploration, the contribution is highlighted by the following.

(1) The 2D Williamson fluid over porous stretching wedge is considered.

(2) The flow is exposed due to suction or injection.

(3) The mixed convection term relating wedge angle Ω is further added in the momentum equation which strengthens the novelty of the recent work.

(4) The chemical reaction equation and Ohmic terms also expand the novelty of the existing work.

(5) Resulting coupled equations with boundary conditions are integrated numerically via the Runge–Kutta (RK) method including shooting scheme through prevalent BCP4C MATLAB built-in function.

(6) Agreement of BVP4C results with the prevailing results available in the literature also improves the novelty of the problem.

2. Model

We investigate 2-dimensional (x, y) mixed convective flow of the Williamson fluid over a wedge. It is presumed that velocity of the possible flow away from boundary layer is $U_\infty = U_0 x^m$. The temperature (T_w) and concentration (C_w) of the wedge are fixed and higher than the ambient concentration and temperature (C_∞, T_∞), respectively (see Figure 1).

The following assumptions are taken into account.

(i) Steady, laminar, incompressible, and mixed convective flow of the Williamson fluid is considered.

(ii) Suction injection is considered at the boundary.

(iii) The chemical reaction is also considered.

(iv) Buoyancy is present in the leading equations.

Within the background of the above-mentioned deductions, the leading equations are as follows [27, 28].

$$\frac{\partial u}{\partial x} + \frac{\partial v}{\partial y} = 0, \tag{1}$$

$$u \frac{\partial u}{\partial x} + v \frac{\partial u}{\partial y} = -\frac{1}{\rho} \frac{\partial p}{\partial x} + \left[v \frac{\partial^2 u}{\partial y^2} \right]$$
$$- \sqrt{2} v \Gamma \frac{\partial u}{\partial y} \frac{\partial^2 u}{\partial y^2} + [\beta_0 g_c (T - T_\infty)$$
$$+ \beta_0 g_c (C - C_\infty)] \sin \frac{\Omega}{2}, \tag{2}$$

$$u \frac{\partial T}{\partial x} + v \frac{\partial T}{\partial y} = -\frac{u}{\rho C_p} \frac{\partial p}{\partial x} + \frac{k}{\rho C_p} \frac{\partial^2 T}{\partial y^2}, \tag{3}$$

$$u \frac{\partial C}{\partial x} + v \frac{\partial C}{\partial y} = D \frac{\partial^2 C}{\partial y^2} - k_1 (C - C_\infty). \tag{4}$$
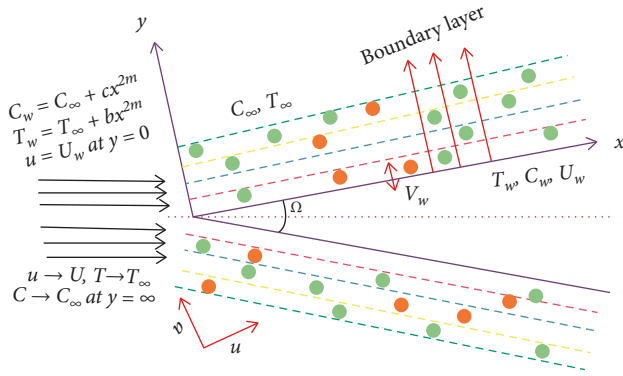
The boundary conditions are

FIGURE 1: Physical model of the problem.

$$u(x, 0) = U_w,$$

$$v(x, 0) = v_w,$$ (5)

$$T(x, 0) = T_w,$$

$$u(x, \infty) = U,$$
$$T(x, \infty) = T_\infty,$$ (6)
$$C(x, \infty) = C_\infty,$$

$$U = U_0 x^m,$$
$$T_w = T_\infty + bx^{2m},$$
$$U_w = RU,$$ (7)
$$v_w = -C(\nu U_0)^{1/2}\left(\frac{m+1}{2}\right)x^{(m-1)/2},$$
$$C_w = C_\infty + cx^{2m},$$

The velocity components u and v take the form

$$u = Uf',$$

$$\eta = \sqrt{U}\, y (\nu x)^{-(1/2)},$$

$$\psi = (\nu x U)^{1/2} f(\eta),$$

$$v = -\sqrt{\nu U_0}\, x^{(m-1)/2}\left[\frac{m+1}{2}f + \frac{m-1}{2}\eta f'\right],$$ (8)

$$h(\eta) = \frac{T - T_\infty}{T_W - T_\infty},$$

$$g(\eta) = \frac{C - C_\infty}{C_W - C_\infty},$$

where stream function ψ defines

$$u = \frac{\partial \psi}{\partial y},$$
$$v = -\frac{\partial \psi}{\partial x},$$ (9)

The above expression also satisfies the continuity equation (1). From (2), (3), and (4), we have the transformed equations

$$\frac{d^3 f}{d\eta^3} - W_e \frac{d^3 f}{d\eta^3}\left(\frac{d^2 f}{d\eta^2}\right) + \frac{1+m}{2} f \frac{d^2 f}{d\eta^2}$$
$$+ m\left[1 - \left(\frac{df}{d\eta}\right)^2\right] + \lambda_1 [h + Ng]\mathrm{Sin}\frac{\Omega}{2} = 0,$$ (10)

$$\frac{1}{\mathrm{Pr}} \frac{d^2 h}{d\eta^2} + \frac{1+m}{2} f \frac{dh}{d\eta} - 2mh\frac{df}{d\eta} + mEc\frac{df}{d\eta} = 0,$$ (11)

$$\frac{d^2 g}{d\eta^2} - K_1 S_c g - S_c\left(2mg\frac{df}{d\eta} - \frac{1+m}{2}f\frac{dg}{d\eta}\right) = 0,$$ (12)

The transformed velocity boundary conditions (5) and (6) can be written as

$$f(0) = C_1,$$
$$f'(0) = R,$$ (13)
$$f'(\infty) = 1,$$

$$h(0) = 1,$$
$$h(\infty) = 0,$$ (14)
$$g(0) = 1,$$
$$g(\infty) = 0,$$

Here, primes signify the differentiation w.r.t η, G_{rx}, λ, S_c, and K_1, these are defined by

$$G^* r_x = \frac{g\beta_c (C_W - C_\infty)x^3}{\nu^2},$$

$$Gr_x = \frac{g\beta_0 (T_W - T_\infty)x^3}{\nu^2},$$

$$N = \frac{Gr_x^*}{Gr_x},$$

$$\mathrm{Re}_x = \frac{Ux}{\nu},$$

$$Ec = \frac{U^2}{C_p (T_W - T_\infty)},$$

$$\mathrm{Pr} = \frac{\mu C_p}{k},$$ (15)

$$\lambda = \frac{Gr_x}{\mathrm{Re}_x^2},$$

$$Sc = \frac{\nu}{D},$$

$$K_1 = \frac{k_1}{Ux},$$

$$\lambda^* = \frac{G^* r_x}{\mathrm{Re}_x^2},$$

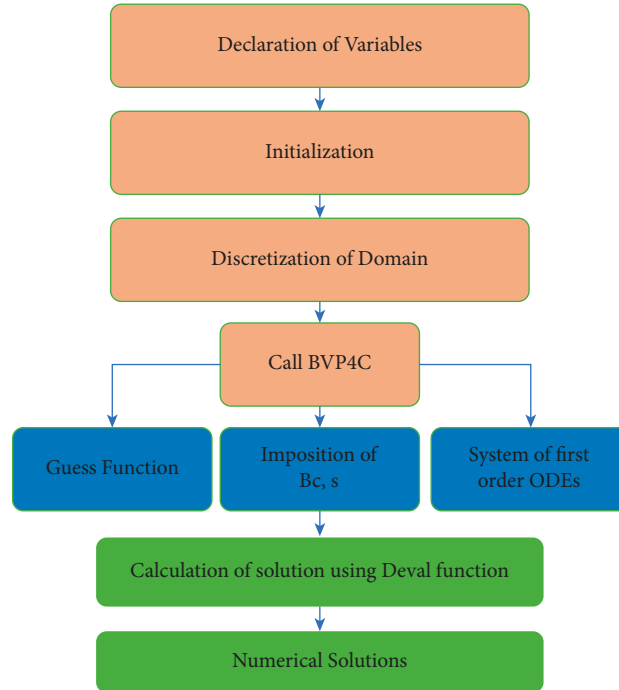$$We = \frac{\sqrt{2}\Gamma U^{3/2}}{\sqrt{\nu x}}.$$

FIGURE 2: Flowchart of the problem.

The quantities of engineering interest are the skin friction coefficient C_f and the Sherwood number Sh_x which are defined by $C_f = \tau_w/\rho U^2$ and $Sh_x = -x\,D\,(\partial C/\partial y)_{y=0}/(C - C_\infty)$ where $\tau_w = \mu\,(\partial u/\partial y)_{y=0}$. With the use of similarity variables, we obtained

$$C_f = \frac{f'(0) + We\,(f'(0))^2}{\sqrt{R_{e_x}}},$$

$$\frac{N_{u_x}}{\sqrt{R_{e_x}}} = -h'(0), \qquad\qquad (16)$$

$$\frac{Sh_x}{\sqrt{R_{e_x}}} = -g'(0).$$

3. Numerical Method and Verification of Code

Dimensionless equations (10), (11), and (12) corresponding to boundary conditions (13) and (14) have been solved using the BVP4C scheme. The solution for the flow over the wedge is obtained using MATLAB software with Core i7 processor. The flowchart is provided in Figure 2. To confirm the validity of the existing numerical system, we have matched the numerical outcomes through those provided by Su et al. [27], Yih [29], and Ishak et al. [30] on the distribution of C_1 for surface drag force of the stretched porous wedge and accomplished an identical decent agreement. Table 1 demonstrates that our consequences are well validated.

4. Discussion

This section highlights the impact of active parameters like flow parameter m, ratio of mixed convective parameter N,

Prandtl and Eckert numbers Pr, Ec, suction injection parameter, velocity ratio parameter R, Schmidt number S_c, and chemical reaction parameter K_1 on velocity f', temperature h, concentration g, skin factor, and heat and mass transfer rate, via graphs. Solid and dashed lines represent when wedge stretches faster or slower than free stream velocity. The black, red, and blue lines represent the velocity, temperature, and concentration fields. Figure 3 is plotted to explore the effect of We on f', h, and g. It is vivid from this figure that the larger values of We increase the temperature and concentration fields and decrease velocity profile. Figure 4 depicts the impact of m on f', g, and h. From this figure, it is found that g and h are minimized while enriching the values of m, but f' lessens at $R = 1.2$ and increases at $R = 0.8$. The graph in Figure 5 shows that N results in decline in g and h, whereas an opposite behavior is noted in $f\prime$ for the values of N.

Figure 6 exhibits the influence of Ec on the three flow fields. At $R = 0.8$, a growing tendency is described for larger values of Ec similar to h and g fields. There is a decay at $R = 1.2$ in the profiles of velocity. Physically, the Eckert number represents the flow of the kinetic energy relative to the enthalpy difference through the thermal boundary layer. The effects of C_1 on f', h, and g are demonstrated in Figure 7. From this figure, it is noted that there is a decay in all the velocity profiles for bigger values of suction injection parameter. The impact of S_c for distinct values of R is drawn in Figure 8. The growing values of S_c decrease the concentration profiles. Figure 9 portrays the values of K_1 (chemical reaction parameter). For constructive or destructive values of chemical reaction parameter, g decreases.

The variations of m and N of C_f against λ_1 are represented in Figure 10. It is found that C_f shows an increasing

TABLE 1: Validated (comparative) values of $f''(0)$ for various choices of C_1.

Value	$\leftarrow C_1 \longrightarrow$				
	1.0	-1.0	-1.5	0.0	0.5
DTM-BF [27]	1.889283054	0756379208	0.969357017	1.233501042	1.541985282
Numerical [29]	1.88931	0.75658	0.96923	1.23259	1.54175
Numerical [30]	1.8893	0.7566	0.9692	1.2326	1.5418
BVP4C results	1.889312724	0.756574914	0.969229200	1.2325863187	1.54175051146
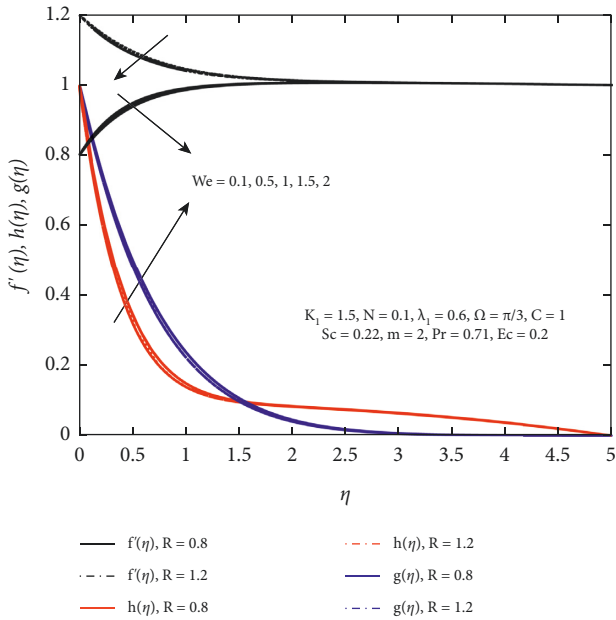
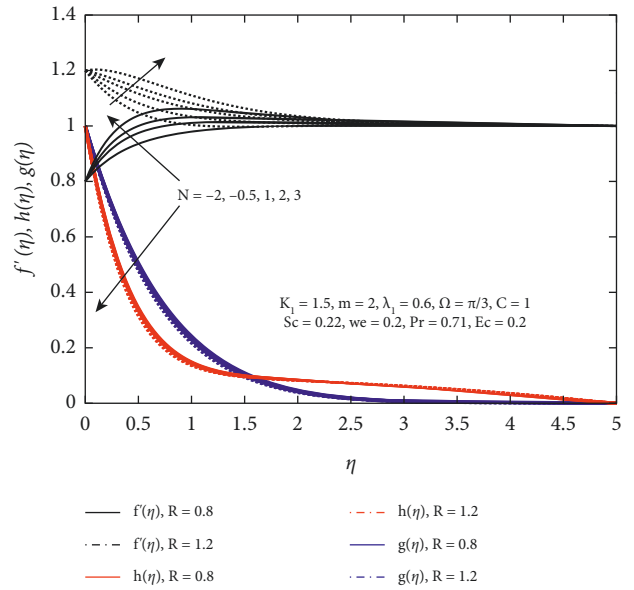FIGURE 3: $f'(\eta), h(\eta), g(\eta)$ for increasing values of We.

FIGURE 5: $f'(\eta), h(\eta), g(\eta)$ for growing values of N.

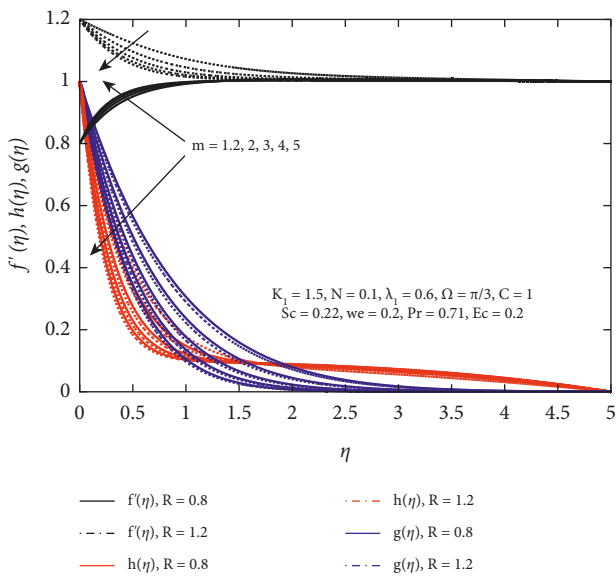
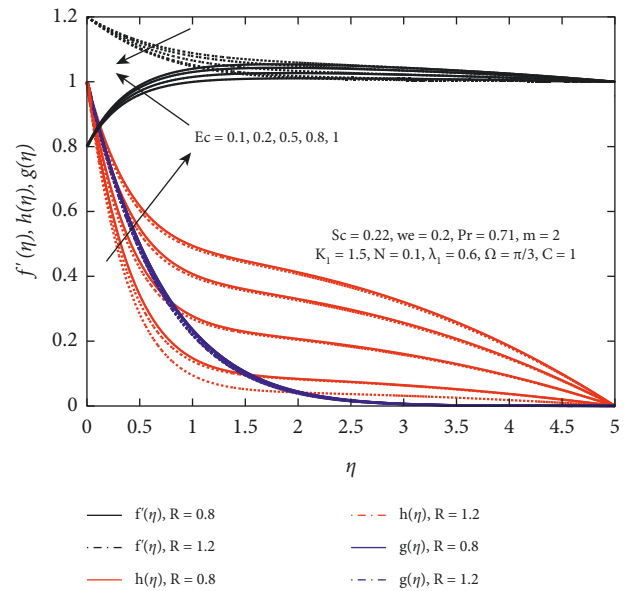FIGURE 4: $f'(\eta), h(\eta), g(\eta)$ for increasing values of m.

FIGURE 6: $f'(\eta), h(\eta), g(\eta)$ for growing values of Ec.

behavior of uplifted values of N, but a reverse behavior is noted for uplifted values of m. Figure 11 shows the influences of S_c and We on C_f. It is noted that C_f increases for augmented values of We and decreases for Sc values. The combined effects of m and N on heat transfer coefficient are depicted in Figure 12. From this figure, N_{u_x} increases for escalating values of N and m. Figure 13 elucidates N_{u_x} for
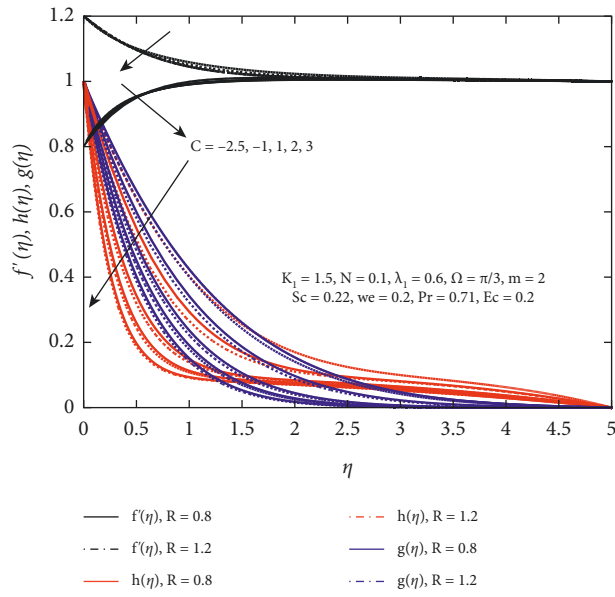
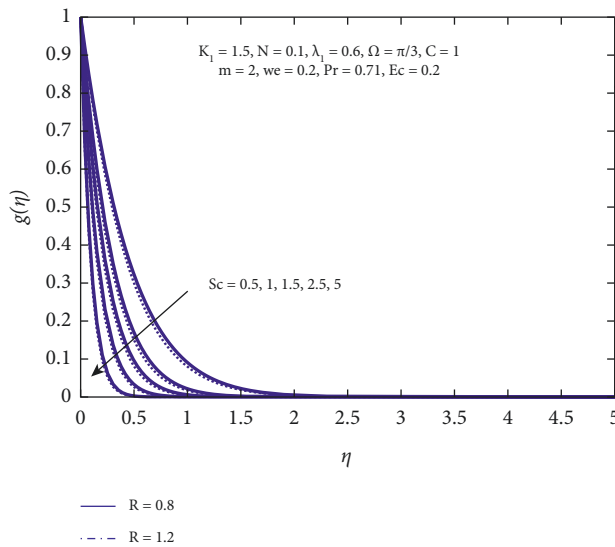FIGURE 7: $f'(\eta), h(\eta), g(\eta)$ for growing values of C_1.

FIGURE 8: $g(\eta)$ for growing values of Sc.
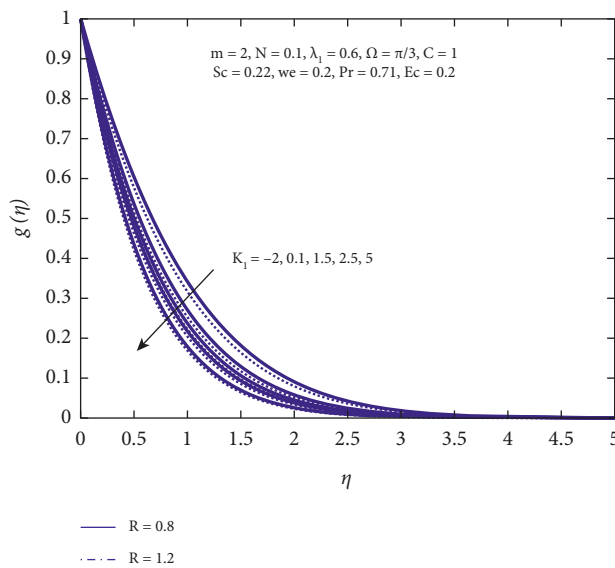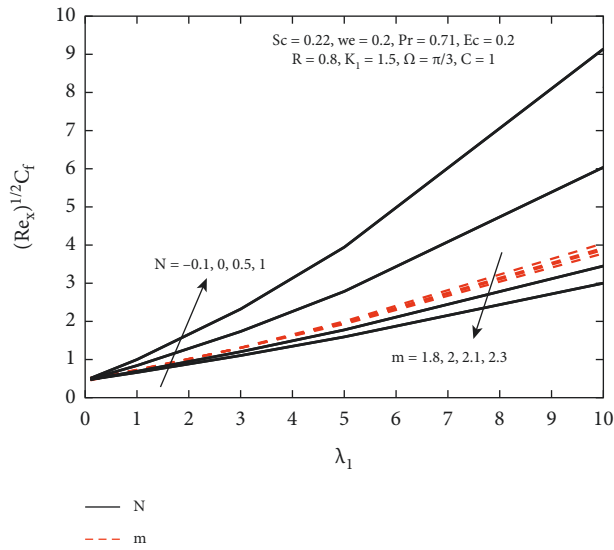

FIGURE 9: $g(\eta)$ for growing values of K_1.

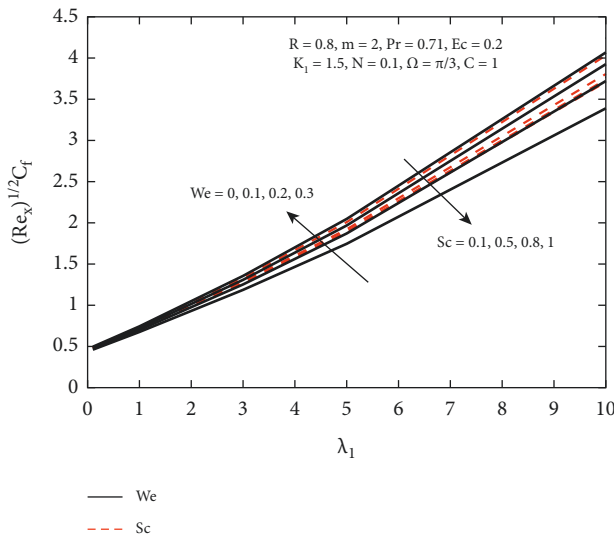FIGURE 10: $C_f \sqrt{R_{ex}}$ against λ_1.

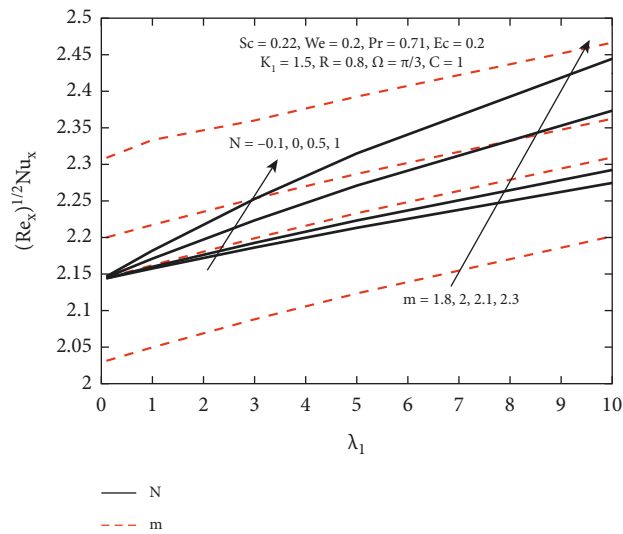FIGURE 11: $C_f \sqrt{R_{ex}}$ for increasing values of Sc and We.

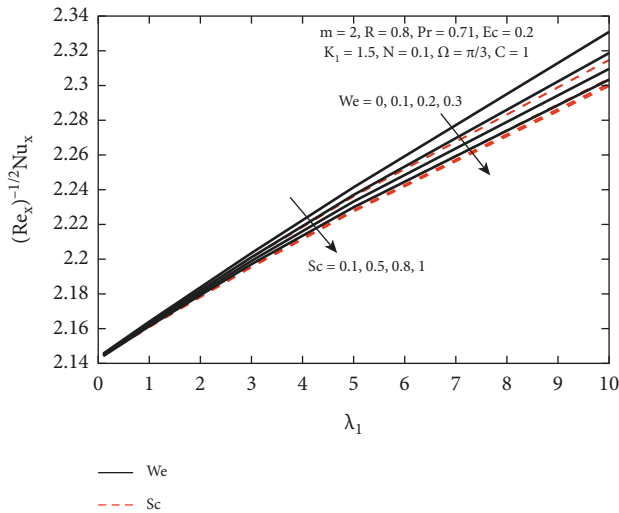FIGURE 12: $N_{ux}/\sqrt{R_{ex}}$ for growing values of N and m.

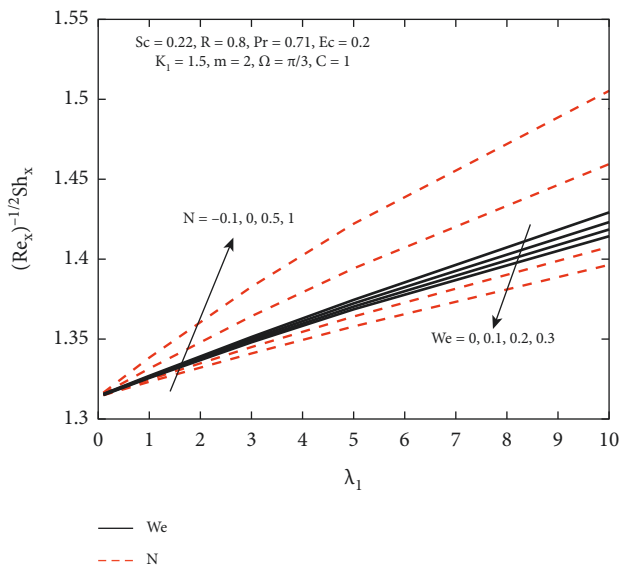FIGURE 13: $N_{ux}/\sqrt{R_{ex}}$ for growing values of We and Sc.

FIGURE 14: $Sh_x/\sqrt{R_{ex}}$ for growing values of We and N.

varied values of We and Sc. Figure 14 is sketched to see the influence of N and We on the rate of mass transfer. Sh_x increases with increasing values of N, and an opposite trend is noted for We.

5. Conclusions

This study was carried out to investigate the chemical reaction and suction/injection effects on Williamson fluid over a porous wedge. The Williamson model, a non-Newtonian model, was used to explore the flow characteristics in the existence of buoyancy and heat transfer. The BVP4C scheme is implemented to elucidate the governing flow equations. These outcomes are demonstrated graphically. From present analysis, the key findings are listed below.

(i) The Weissenberg number surges up the temperature and concentration velocity, whereas it reduces the fluid velocity.

(ii) Larger values of m and N escalate the rate of mass transfer.

(iii) A rise in We and Sc enhances the rate of heat transfer.

(iv) We and Sc numbers on skin friction are reverse in nature.

(v) Mass transfer rate escalates for N and declines for We.

Nomenclature

W_e:	Weissenberg number
R:	Velocity ratio parameter
f':	Dimensionless velocity
C:	Concentration velocity
(x, y):	Coordinates (m)
g:	Dimensionless concentration velocity
h:	Dimensionless temperature velocity
(u, v):	Velocity component (ms^{-1})
T_w:	Wall temperature
C_w:	Wall concentration
m:	Flow parameter
T:	Temperature of the fluid
C_∞:	Concentration of free stream
T_∞:	Temperature of free stream
u_w:	Stretching velocity (ms^{-1})
v:	Fluid kinematic viscosity
C_p:	Specific heat (J K^{-1} kg^{-1})
g_c:	Gravitational acceleration
S_c:	Schmidt number
k:	Thermal conductivity of the fluid (W K^{-1} m^{-1})
C_1:	Suction/injection parameter
K_1:	Chemical reaction parameter
E_c:	Eckert number
U:	Free stream velocity
G_r:	Grashof number
R_e:	Reynolds number
μ:	Fluid dynamic viscosity (pas)
λ:	Mixed convection parameter
ρ:	Density of fluid (kg m^{-3})
β_0:	Thermal expansion coefficient
η:	Similarity variable
σ:	Electrical conductivity of the fluid
Ω:	Wedge angle parameter
ODEs:	Ordinary differential equations

PDEs: Partial differential equations
BCs: Boundary conditions
RK: Runge–Kutta
3D: Three-dimensional
2D: Two-dimensional.

Data Availability

No data were used to support this study.

Conflicts of Interest

The authors declare that they have no conflicts of interest.

Authors' Contributions

All authors jointly worked on the results, and they have read and approved the final version of the manuscript.

References

[1] K. Aurangzaib, S. S. Bhattacharyya, K. Bhattacharyya, and S. Shafie, "Effect of partial slip on an unsteady MHD mixed convection stagnation-point flow of a micropolar fluid towards a permeable shrinking sheet," *Alexandria Engineering Journal*, vol. 55, no. 2, pp. 1285–1293, 2016.

[2] M. Bibi, M. Y. Khalil-Ur-Rehman, M. Y. Malik, and M. Tahir, "Numerical study of unsteady Williamson fluid flow and heat transfer in the presence of MHD through a permeable stretching surface," *The European Physical Journal Plus*, vol. 133, no. 4, p. 154, 2018.

[3] S. Hazarika and S. Ahmed, "Brownian motion and thermophoresis behavior on micro-polar nano-fluid-A numerical outlook," *Mathematics and Computers in Simulation*, vol. 192, pp. 452–463, 2022.

[4] E.-A. B. Cavitation, *Non-Newtonian Fluids: With Biomedical and Bioengineering Applications,* Springer-Verlag, Berlin Heidelberg, 2011.

[5] R. V. Williamson, "The flow of pseudoplastic materials," *Industrial & Engineering Chemistry*, vol. 21, no. 11, pp. 1108–1111, 1929.

[6] M. Y. Malik, M. Bibi, F. Khan, and T. Salahuddin, "Numerical solution of Williamson fluid flow past a stretching cylinder and heat transfer with variable thermal conductivity and heat generation/absorption," *AIP Advances*, vol. 6, no. 3, Article ID 035101, 2016.

[7] G. Kumaran, N. Sandeep, and R. Vijayaragavan, "Melting heat transfer in magnetohydrodynamic radiative Williamson fluid flow with non-uniform heat source/sink," *IOP Conference Series: Materials Science and Engineering*, vol. 263, Article ID 062022, 2017.

[8] T. Hayat, S. Ayub, A. Tanveer, and A. Alsaedi, "Numerical simulation for MHD Williamson fluid utilizing modified Darcy's law," *Results in Physics*, vol. 10, pp. 751–759, 2018.

[9] C. Raju, N. Sandeep, M. Ali, and A. Nuhait, "Heat and mass transfer in 3-D MHD Williamson-Casson fluids flow over a stretching surface with non-uniform heat source/sink," *Thermal Science*, vol. 23, no. 1, pp. 281–293, 2019.

[10] S. Noreen, S. Waheed, D. Lu, and A. Hussanan, "Heat measures in performance of electro-osmotic flow of Williamson fluid in micro-channel," *Alexandria Engineering Journal*, vol. 59, no. 6, pp. 4081–4100, 2020.

[11] K. Subbarayudu, S. Suneetha, and P. Bala Anki Reddy, "The assessment of time dependent flow of Williamson fluid with radiative blood flow against a wedge," *Propulsion and Power Research*, vol. 9, no. 1, pp. 87–99, 2020.

[12] Z. Hussain, T. Hayat, A. Alsaedi, and I. Ullah, "On MHD convective flow of Williamson fluid with homogeneous-heterogeneous reactions: a comparative study of sheet and cylinder," *International Communications in Heat and Mass Transfer*, vol. 120, Article ID 105060, 2021.

[13] T. Salahuddin, M. Khan, T. Saeed, M. Ibrahim, and Y.-M. Chu, "Induced MHD impact on exponentially varying viscosity of Williamson fluid flow with variable conductivity and diffusivity," *Case Studies in Thermal Engineering*, vol. 25, Article ID 100895, 2021.

[14] S. Ahmed, A. Batin, and A. J. Chamkha, "Numerical/Laplace transform analysis for MHD radiating heat/mass transport in a Darcian porous regime bounded by an oscillating vertical surface," *Alexandria Engineering Journal*, vol. 54, no. 1, pp. 45–54, 2015.

[15] S. Hazarika, S. Ahmed, and A. J. Chamkha, "Investigation of nanoparticles Cu, Ag and Fe3O4 on thermophoresis and viscous dissipation of MHD nanofluid over a stretching sheet in a porous regime: a numerical modeling," *Mathematics and Computers in Simulation*, vol. 182, pp. 819–837, 2021.

[16] R. Zahmatkesh, H. Mohammadiun, M. Mohammadiun, and M. H. Dibaei Bonab, "Investigation of entropy generation in nanofluid's axisymmetric stagnation flow over a cylinder with constant wall temperature and uniform surface suction-blowing," *Alexandria Engineering Journal*, vol. 58, no. 4, pp. 1483–1498, 2019.

[17] K. Singh, A. K. Pandey, and M. Kumar, "Slip flow of micropolar fluid through a permeable wedge due to the effects of chemical reaction and heat source/sink with Hall and ion-slip currents: an analytic approach," *Propulsion and Power Research*, vol. 9, no. 3, pp. 289–303, 2020.

[18] A. Mustaffa Saleem, N. Moner Basher, and A. Ahmed Yousif, "Effect of suction or blowing on velocity and temperature distribution of flow over a flat plate," *Materials Today Proceedings*, vol. 42, pp. 2859–2865, 2021.

[19] D. F. Fairbanks and C. R. Wilke, "Diffusion coefficients in multicomponent gas mixtures," *Industrial & Engineering Chemistry*, vol. 42, no. 3, pp. 471–475, 1950.

[20] S. Ahmed, K. Kalita, and A. J. Chamkha, "Analytical and numerical solution of three-dimensional channel flow in presence of a sinusoidal fluid injection and a chemical reaction," *Ain Shams Engineering Journal*, vol. 6, no. 2, pp. 691–701, 2015.

[21] C. Sulochana, A. G. Poojari, and N. Sandeep, "Effect of frictional heating on mixed convection flow of chemically reacting radiative Casson nanofluid over an inclined porous plate," *Alexandria Engineering Journal*, vol. 57, no. 4, 2017.

[22] A. Zaib, M. M. Rashidi, A. J. Chamkha, and K. Bhattacharyya, "Numerical solution of second law analysis for MHD Casson nanofluid past a wedge with activation energy and binary chemical reaction," *International Journal of Numerical Methods for Heat and Fluid Flow*, vol. 27, pp. 2816–2834, 2017.

[23] S. Nandi and B. Kumbhakar, "Viscous dissipation and chemical reaction effects on Tangent hyperbolic nanofluid flow past a stretching wedge with convectiv heating and Navier's slip conditions," *Iranian J Science and Tech, Trans of Mech Enging*, 2011.

[24] H. Waqas, U. Farooq, S. A. Khan, H. M. Alshehri, and M. Goodarzi, "Numerical analysis of dual variable of conductivity in bioconvection fow of Carreau--Yasuda nanofuid

containing gyrotactic motile microorganisms over a porous medium," *Journal of Thermal Analysis and Calorimetry*, vol. 145, 2021.

[25] T. Mushtaq, A. Rauf, S. A. Shehzad, F. Mustafa, M. Hanif, and Z. Abbas, "Numerical and statistical approach for Casson-Maxwell nanofluid flow with Cattaneo-Christov theory," *Applied. Mathematics.Mechanics*, vol. 42, 2021.

[26] S. Hazarika and S. Ahmed, "Theoretical investigation of viscosity and thermal conductivity of a gas along a non-isothermal vertical surface in porous environment with dissipative heat: numerical technique," *Journal of Applied and Computational Mechanics*, pp. 1–10, 2021.

[27] X. Su, L. Zheng, X. Zhang, and J. Zhang, "MHD mixed convective heat transfer over a permeable stretching wedge with thermal radiation and ohmic heating," *Chemical Engineering Science*, vol. 78, pp. 1–8, 2012.

[28] V. Rajesh, M. A. Sheremet, and H. F. Öztop, "Impact of hybrid nanofluids on MHD flow and heat transfer near a vertical plate with ramped wall temperature," *Case Studies in Thermal Engineering*, vol. 28, Article ID 101557, 2021.

[29] K. A. Yih, "MHD forced convection ‡ow adjacent to a non-isothermal wedge," *International Communications in Heat and Mass Transfer*, vol. 26, pp. 819–827, 1998.

[30] A. Ishak, R. Nazar, and I. Pop, "Falkner-Skan equation for flow past a moving wedge with suction or injection," *Journal of Applied Mathematics and Computing*, vol. 25, no. 1-2, pp. 67–83, 2007.